Alma Mater Studiorum Università di Bologna
Archivio istituzionale della ricerca

Thermal behavior of Carrara marble after consolidation by ammonium phosphate, ammonium oxalate and ethyl silicate

(Article begins on next page)

10 March 2025

THERMAL BEHAVIOR OF CARRARA MARBLE AFTER CONSOLIDATION BY AMMONIUM PHOSPHATE, AMMONIUM OXALATE AND ETHYL SILICATE

Enrico Sassoni[1], Gabriela Graziani[1,*], Giovanni Ridolfi[2], Maria Chiara Bignozzi[1,2], Elisa Franzoni[1]

[1] Department of Civil, Chemical, Environmental and Materials Engineering (DICAM),

University of Bologna, Via Terracini 28, 40131, Bologna (Italy)

[2] Centro Ceramico, via Martelli 26, Bologna, Italy

* Corresponding Author

Tel: +39 051 2090323, Fax: +39 051 2090322, e-mail: gabriela.graziani2@unibo.it

ABSTRACT

The response to thermal variations is the primary cause of marble deterioration in ancient and modern buildings. In this study, the thermal behavior of Carrara marble after consolidation by an innovative hydroxyapatite-based treatment was investigated in comparison with ammonium oxalate and ethyl silicate. Samples were subjected to heating-cooling cycles up to 80 °C. All the consolidating treatments were found to be fairly compatible, as in no case the residual strain after the thermal cycles was found to increase compared to the unweathered untreated marble. Anyway, the hydroxyapatite-treatment has the advantage of causing the highest increase in marble cohesion and the lowest residual strain, besides being more chromatically compatible and durable than the alternative commercial consolidants.

KEYWORDS

Hydroxyapatite; Calcium oxalate; Thermal expansion coefficient; Residual strain; Dilatometry

1. INTRODUCTION

Thermal excursions, such as day/night temperature variations and heating/cooling cycles due to exposure to solar radiation, are known to be the primary cause of deterioration of marble used for decorating historic buildings and for cladding modern façades. Thermal deterioration originates from the anisotropic thermal behavior of calcite crystals constituting marble [1]. Upon heating, calcite crystals expand parallel and contract perpendicular to the crystallographic c-axis, thus generating stress inside marble. When stress exceeds the cohesion among calcite grains, new (i.e. previously not existing) micro-cracks are formed at grain boundaries [1,2]. These newly developed micro-cracks progressively lead to two characteristic deterioration phenomena affecting marble: the so-called "sugaring" (i.e., grain detachment and loss) [3,4] and the bowing of thin slabs used as gravestones or cladding elements [5,6], as illustrated in Figure 1. Sugaring and bowing are major issues threatening the durability of both historic monuments (e.g. the Cathedral of Florence and the Alhambra Palace in Granada) and modern buildings (e.g. the New York Public Library and the Finland Hall by Alvar Aalto in Helsinki) [3]. Besides causing the loss of important historic artifacts, these weathering phenomena also have significant economic consequences: for instance, the replacement of the bowed slabs used for cladding the Amoco Building in Chicago cost as much as $ 65 million [1]. In addition, thermally induced micro-cracks increase marble porosity and surface area, which results in increased marble susceptibility to dissolution in rain [7], black crust formation [8] and deterioration due to salt crystallization [9].

To re-establish cohesion between loose calcite grains, numerous organic and inorganic consolidating treatments have been proposed through the years [3,9-16]. In spite of the relatively abundant literature on consolidants effects on marble mechanical and sorption properties, a very limited number of studies investigated how consolidants affect marble thermal behavior [8,17]. Considering that marble response to temperature variations is the primary cause of its deterioration, the possible change in thermal behavior after consolidation is one of the most important aspects to

evaluate the suitability of any possible consolidant for marble. In fact, in case the applied treatment was found to worsen marble thermal behavior, consolidation would result being counterproductive. For instance, this was the case of an organic consolidant based on polymethyl-methacrylate dissolved in xylenes, found to significantly increase marble residual strain after thermal cycles, thus potentially leading to accelerated deterioration [17].

The present study is aimed at evaluating the thermal behavior of weathered Carrara marble after consolidation with an innovative treatment based on hydroxyapatite. This treatment, originally proposed for limestone consolidation [18], is based on the formation of hydroxyapatite ($Ca_{10}(PO_4)_6(OH)_2$, HAP) from the reaction between calcite grains and an aqueous solution of diammonium hydrogen phosphate (($NH_4)_2HPO_4$, DAP) [18,19]. The HAP-treatment has recently been investigated for consolidation of sugaring marble and very encouraging results have been obtained. Indeed, the HAP-treatment proved to restore weathered marble cohesion back to the condition before weathering, without significantly altering marble color [16]. The HAP-treatment outperformed traditional consolidants (such as ammonium oxalate and ethyl silicate), thus standing out as one of the most promising inorganic treatments for marble preservation [16]. In addition to the good consolidating ability, the HAP-treatment is also able to improve marble resistance to dissolution in rain, thanks to the very low solubility and slow dissolution rate of HAP, compared to calcite [19,20]. Considering its high potential, further development of the HAP-treatment for consolidation and protection of marble and limestone has been undertaken by several research groups [18-30] and the European Commission has recently funded the Marie Skłodowska-Curie project "HAP4MARBLE" [31], specifically aimed at multi-functionalizing the HAP-treatment for marble restoration and preventive conservation.

The issue of how HAP-consolidated marble responds to thermal stress has been preliminarily addressed by the Authors in a previous study [32]. An accelerated procedure, consisting in heating samples at 400 °C for 1 hour, was adopted to cause thermal damage in consolidated marble, whose response was evaluated in terms of loss of consolidating efficacy [32].

Such heating procedure is effective in rapidly causing micro-cracks in marble (which can be exploited also for producing decayed samples suitable for testing of consolidants [33,34]), however it was found to be too extreme to evaluate the response that consolidated marble has in the field when subjected to natural thermal excursions (rarely exceeding a maximum temperature of ~80 °C [8]). Therefore, in the present study, conditions much closer to the real ones were adopted (heating-cooling cycles up to 80 °C), so that the actual thermal behavior of HAP-consolidated marble could be assessed. For comparison's sake, marble thermal behavior after treatment with ammonium oxalate and ethyl silicate (the two inorganic treatments most widely used nowadays in the practice of marble consolidation [35,36]) was evaluated as well. To the Authors' best knowledge, the present study is the first attempt to evaluate the thermal behavior of marble consolidated by HAP and ammonium oxalate, whereas one study on the thermal behavior of marble treated with ethyl silicate has been reported in the literature [17].

2.   MATERIALS AND METHODS

2.1   Marble samples

A freshly quarried slab of White Carrara marble (supplied by Imbellone Michelangelo s.a.s., Italy) was used. From the slab, 12 prismatic samples ($30 \times 30 \times 20$ mm^3) were wet sawn. Two samples were left unweathered and untreated (samples labeled "UW-UT"), while samples to be consolidated by different treatments were subjected to preliminary artificial weathering. Indeed, as pointed out by several studies, testing consolidants on unweathered marble leads to unreliable results, because of its very low porosity and the consequent very low consolidant penetration into the unweathered substrate [10,16,32]. Hence, preliminary artificial weathering was performed by heating samples in oven at 400 °C for 1 hour, according to a method previously developed by the Authors [33,34]. After heating at high temperature, marble samples exhibit formation of new micro-cracks, increase in open porosity and coarsening of pore radius very similar to those exhibited by naturally

weathered marbles [3,16]. After artificial weathering, two samples were left untreated (samples labeled "W-UT"), while the remaining samples were subjected to different consolidating treatments (two samples per treatment), as described in the following.

2.2   Consolidating treatments

Two different formulations of the HAP-treatment were tested and compared with ammonium oxalate and ethyl silicate, for a total of 4 investigated treatments. All the treatments were applied to the previously weathered samples (W- prefix in the relevant labels), for the reasons explained above.

2.2.1   DAP 3 M

The first formulation of the HAP-treatment was that proposed in [16], involving marble treatment with a 3 M aqueous solution of DAP, followed by application of a poultice impregnated with limewater (i.e. a saturated $Ca(OH)_2$ solution). The samples (labeled "W-DAP3M") were firstly treated with a 3 M aqueous solution of DAP (Sigma-Aldrich, reagent grade), applied by brushing on a 30×30 mm^2 face until apparent refusal (8 brush strokes). At the end of the brushing application, the samples were wrapped in a plastic film to avoid evaporation and left to react for 48 hours, then unwrapped, rinsed with water and left to dry in laboratory conditions (T=20±2 °C, RH=50±5%) until constant weight. Then, samples were further treated with a limewater poultice (weight ratio between dry cellulose pulp and limewater 1:6). As discussed more in detail in previous studies [16,37], the application of the limewater poultice has the double beneficial effect of supplying additional calcium ions for reaction with unreacted DAP (that is still present 48 hours after the treatment [16]) and removing soluble phases during poultice drying (so that still unreacted DAP finally crystallizes in the poultice, instead of over marble surface). After application of the limewater poultice (using a sheet of Japanese paper between the sample and the poultice to avoid

sticking), samples were wrapped in a plastic film to avoid limewater evaporation and left to react for 24 hours, then unwrapped and left to dry in laboratory conditions with the poultice in contact with the samples. Then, samples were rinsed with water to remove poultice residues and left to dry in laboratory conditions.

2.2.2   DAP 0.1 M

The second formulation of the HAP-treatment was that recently proposed in [21], involving a two-step treatment with a 0.1 M DAP aqueous solution, also containing ethanol during the first step. As suggested in [21] and discussed more in detail in [38], the addition of ethanol makes it possible to reduce the concentration of the DAP solution to a value as low as 0.1 M (for which no calcium phosphate phases are formed in absence of ethanol). A reduction in the DAP concentration is expected to have the positive effect of reducing the thickness of the HAP layer formed over calcite grains, thus reducing its tendency to crack during drying. Moreover, the addition of ethanol to the DAP solution has also the beneficial effect of reducing the porosity of the HAP coating, which is expected to be improve the treatment performance as well [38]. The samples (labeled "W-DAP0.1M") were firstly treated with a 0.1 M aqueous solution of DAP, also containing 0.1 mM $CaCl_2$ and 0.5 wt% ethanol, applied by immersion for 24 hours (the beaker containing the solution being sealed with a plastic film). The W-DAP0.1M samples were treated by immersion (and not by brushing like the W-3M DAP samples) because of ethanol presence. Since ethanol is highly volatile, the behavior of the ethanol-containing DAP solution when applied by brush needs to be specifically investigated, in terms of competition between the organic solvent evaporation and the solution penetration inside marble. This is beyond the scope of the present paper, therefore application by immersion was performed, so that any ethanol evaporation was prevented. After immersion for 24 hours, samples were rinsed with water and ethanol and left to dry in laboratory conditions until constant weight. Afterwards, samples were subjected to a second treatment, performed exactly as the first one, except for ethanol addition to the DAP solution (ethanol was not

added during the second treatment to avoid excessive thickening and cracking of the HAP layer formed over calcite [21]). At the end of the second treatment, samples were rinsed and left to dry in laboratory conditions.

2.2.3 Ammonium oxalate

The treatment is based on formation of calcium oxalate as the reaction product between calcite and ammonium oxalate [39]. The samples (labeled as "W-AmOx") were treated with a 5 wt% aqueous solution of ammonium oxalate (Sigma-Aldrich, reagent grade), applied by brushing on a 30×30 mm^2 face until apparent refusal (15 brush strokes). At the end of the brushing application, the samples were wrapped in a plastic film to avoid evaporation and left to react for 48 hours, then unwrapped, rinsed with water and left to dry in laboratory conditions until constant weight.

2.2.4 Ethyl silicate

The treatment is based on formation of amorphous silica from the hydrolysis-condensation reactions of ethyl silicate that stone is impregnated with. The samples (labeled as "W-ES") were treated with the commercial product Estel 1000 by CTS s.r.l. (Italy), composed of 75 wt% ethyl silicate (also containing 1% dibutyltin dilaurate as catalyst) and 25 wt% white spirit, applied on a 30×30 mm^2 face by brushing until apparent refusal (8 brush strokes). The samples were cured for 1 month in laboratory conditions. Afterwards, curing completion was achieved by a novel method recently proposed by the Authors, allowing hydrophobicity to be fully lost and mechanical improvement to be fully reached in a much accelerated way [40]. A water poultice (weight ratio between dry cellulose pulp and water 1:6) was applied to the samples for 4 days (evaporation being impeded by wrapping in a plastic film), then samples were rinsed with water and left to dry in laboratory conditions until constant weight.

2.3   Characterization

2.3.1   *Consolidating ability*

The effectiveness of the different consolidating treatments was evaluated by measuring the increase in ultrasonic pulse velocity (*UPV*) after consolidation. The *UPV* is very sensitive to the formation and healing of micro-cracks inside marble and can be measured by a non-destructive technique, hence it is frequently adopted to assess the state of conservation of marble [41,42]. The *UPV* was measured on two prismatic samples ($30\times30\times20$ mm^3) for each condition. A Matest instrument with 55 kHz transducers was used to test the samples by transmission method parallel to the 20 mm side, using a rubber couplant between the sample and the transducers to improve the contact. After *UPV* measurement, one prismatic sample for each condition was used to obtain specimens for scanning electron microscopy (SEM) and mercury intrusion porosimetry (MIP), while the other sample was used to obtained specimens for dilatometry, as described in the following.

SEM observation was performed on one fracture sample for each condition, to qualitatively evaluate the formation of new micro-cracks after artificial weathering and their healing after consolidation. A scanning electron microscope LEO "EVO 40XVP-M" Zeiss was used, after making the samples conductive by carbon coating.

MIP analysis was carried out on one sample for each condition, obtained by chisel from the first 5 mm from the treated surface, to quantitatively assess the effect of artificial weathering and consolidation on micro-cracks volume and size. A Carlo Erba Porosimeter 2000 with a Fisons Macropore Unit 120 was used.

2.3.2   *Thermal behavior*

The thermal behavior of untreated and treated samples was assessed by dilatometry on duplicate specimens ($30\times9\times7$ mm^3), both sawn from one of the $30\times30\times20$ mm^3 samples previously used for measuring the *UPV*. The samples were obtained near the treated surface, so that the maximum

depth from the treated surface was the 9 mm side. Samples were subjected to two heating-cooling cycles, using a push-rod dilatometer Netzsch 402E (Netzsch-Geratebäu GmbH, Selb, Germany), calibrated with NIST SRM 731 borosilicate glass. Each cycle consisted in heating from room temperature to 80 °C at 1 °C /min, holding at 80 °C for 1 hour and then cooling to room temperature at 1 °C /min. The maximum heating temperature of 80 °C was selected to reproduce conditions similar to those encountered in the field [8,17]. The maximum strain registered at 80 °C (ε_{max}, in mm/m) and the residual strain after cooling to 35 °C (ε_r, in mm/m) were measured. The reference temperature of 35 °C was selected instead of room temperature, as the latter slightly varied between the tests. During the cooling phase of each cycle, the thermal expansion coefficient (α_t, in °C^{-1}) was measured as $\alpha_t = \Delta L/(L_0 \cdot \Delta T)$, where ΔL is the length variation, L_0 is the initial length and $\Delta T = 25$ °C is the temperature difference between 35 and 60 °C (corresponding to the linear part of the cooling curve, cf. § 3.2).

The formation of new micro-cracks after the heating-cooling cycles was also evaluated by SEM observation, using the same instrument described above. To distinguish between micro-cracks originated by preliminary artificial weathering and new micro-cracks formed during the thermal cycles, the following criterion was used. Micro-cracks containing newly formed consolidating phases were assumed to be cracks originated by preliminary weathering and filled after consolidation, whereas "clean" micro-cracks (containing no consolidant) were assumed to be new cracks originated during the heating-cooling cycles.

3. RESULTS AND DISCUSSION

3.1 Consolidating ability

The modifications in *UPV* after artificial weathering and consolidation are reported in Table 1. Heating at 400 °C caused a 81% decrease in *UPV* (from 3.2 to 0.6 km/s), as a result of new micro-cracks originated by the anisotropic thermal deformation of calcite crystals. The formation of new

micro-cracks is clearly visible by comparing the SEM images of unweathered and weathered samples ("UW-UT-Pre" and "W-UT-Pre" in Figure 2, respectively). As reported in Figure 4, these new micro-cracks resulted in a severe increase in open porosity, from 1.0 (UW-UT) to 5.2% (W-UT).

After consolidation, the W-DAP3M samples exhibited the highest increase in *UPV* (up to 2.9 km/s), so that the mechanical properties were almost completely restored to the original unweathered condition. This *UPV* increase was due to the penetration of the DAP solution all through the sample thickness (as visually assessed at the end of the brushing application) and to the formation of new calcium phosphate phases inside the pre-existing micro-cracks. As can be observed in Figure 3 ("W-DAP3M-Pre"), clusters of new calcium phosphate phases, having the typical flowery morphology, formed over the surface of calcite grains and inside micro-cracks. Even if the treatment did not cause a complete occlusion of the existing micro-cracks (Figure 4, the highest modification being in the volume of pores with size bigger than 10 μm), still the micro-crack tips were efficiently healed by HAP, which resulted in increased cohesion and *UPV*.

The W-DAP0.1M samples exhibited an increase in *UPV* up to 2.2 km/s, hence slightly lower than the W-DAP3M samples (Table 1). The lower *UPV* increase is thought to be due to the lower penetration depth of the consolidating solution into the W-DAP0.1M samples, which probably led to the presence of unhealed micro-cracks deep inside the samples. This is suggested by SEM observation, revealing the formation of significant amounts of HAP inside the micro-cracks in the first millimeters from the surface (Figure 3, "W-3M DAP-Pre" sample), while in the centre of the sample only few traces of the new phases could be found. A possible explanation for this finding is the adopted treating method (immersion in the DAP solution), which might have caused some trapping of air bubbles inside the samples. This suggests that in the future, once the volatility of the ethanol-containing DAP solution has been investigated, the thermal behavior of samples treated by brushing should be evaluated. Notably, the *UPV* increase obtained for the W-DAP0.1M samples was achieved even if these samples were treated with a DAP concentration 30 times lower than the

W-DAP3M samples. This was possible thanks to the addition of ethanol during the first step of the double treatment, because ethanol promotes HAP formation by weakening the hydration shells of ions in solution [21,42,43]. Accordingly, the new phases exhibit a different morphology (Figure 3): more diffused, prismatic agglomerates can be noticed in the W-DAP0.1M samples, compared to the smaller, globular clusters in the W-DAP3M samples.

As reported in Table 1, the W-AmOx samples exhibited an increase in *UPV* up to 2.3 km/s, similar to the W-DAP0.1M samples. The alteration in marble pore size distribution caused by ammonium oxalate was quite limited (Figure 4, mostly in the pores with size bigger than 10 μm), mainly because the penetration depth of this treatment is quite low. As observed by SEM ("W-AmOx-Pre" in Figure 3), formation of calcium oxalate was detected almost exclusively in the most superficial area (about 1-2 mm from the treated surface), while in depth the consolidant was present only in traces and was unable to bind cracks. Scarce penetration depth of the AmOx treatment was also found in previous studies [16].

The W-ES samples experienced the lowest mechanical improvement (*UPV* up to 2.1 km/s), in spite of the good penetration depth (samples were fully saturated at the end of the brushing application and accordingly the consolidant was detected by SEM also in the inner parts of the sample) and in spite of the pronounced pore occlusion (as illustrated in Figure 4, pores with size bigger than 10 μm are completely occluded and those in the range 1-10 μm are diminished). As reported in the literature, the strengthening ability of ethyl silicate is generally limited, as it deposits amorphous silica inside micro-cracks without chemically bonding to calcite grains [44]; in fact, a scarce adhesion between silica gel and calcite grain surfaces could be clearly observed by SEM ("W-ES-Pre" in Figure 3).

3.2   Thermal behavior

The thermal behavior of unweathered, untreated marble (UW-UT condition) is illustrated in detail in Figure 5 for a representative sample. The heating curve is non-linear, the curve concavity

increasing for increasing temperature. The initial part of the curve, having a lower slope, is representative of the intrinsic properties of marble; the second part, having a higher slope, is affected by progressive micro-cracks formation as temperature increases [45]. The average maximum strain (0.69 mm/m at 80 °C, Table 2) fairly agrees with results previously reported in the literature for Carrara marble heated at the same temperature (maximum strain ~0.8 mm/m [1,45]). During the cooling phase, some calcite grains rearrangement takes place, however a remarkable residual strain is present (ε_{res} = 0.26 mm/m, Table 2). This value is again in line with residual strain values previously reported in the literature (~0.2 mm/m) [1,45]. As the sample is re-heated, the curve initially exhibits a slope that is much lower than that during the first heating cycle. This is thought to be a consequence of the new micro-cracks formed during the first cycles and responsible for the residual strain at the end of the first cycle. These micro-cracks allow some deformation of the calcite crystals without causing additional thermal degradation (the so-called "buffering" effect) [17,34]. The re-heating curve then becomes steeper and the slope reaches a value similar to the first heating cycle. The cooling curve during the second cycle is basically parallel to that during the first one, suggesting that the cooling phase is more representative of the intrinsic properties of the material, because (compared to the heating phase) this phase is less affected by thermally induced micro-cracks. For this reason, the thermal expansion coefficient was measured during the cooling phase of each cycle, in the linear part between 35 and 60 °C. Between the first and the second cycle, α_t exhibits a small decrease (from 10.8 to 9.5 × 10^{-6} °C^{-1}, Table 2), due to the presence of some micro-cracks formed during the first cycle and influencing the behavior during the second cycle. At the end of the second cycle, the additional residual strain (with respect to the condition at the end of the first cycle) is sensibly smaller (on average, 0.06 mm/m, while the residual strain at the end of the first cycle was 0.26 mm/m, Table 2). This is again as a consequence of the "buffering" effect allowed by the initial micro-cracks. After the second cycle, the newly developed micro-cracks are clearly visible by SEM (Figure 2, UW-UT-Post).

Weathered, untreated marble (W-UT samples) exhibits a sensibly different behavior compared to unweathered marble. Having been preliminarily damaged by heating at 400 °C, the W-UT samples initially have an open porosity much higher than the UW-UT samples (5.2% instead of 1.0%, Figure 4). This porosity is responsible for a remarkable "buffering" effect, even during the first heating/cooling cycle. This results in a much reduced α_t (3.0 instead of 10.8 °C^{-1}, Table 2) and a much smaller ε_{res} (0.10 instead of 0.26 mm/m, Table 2). During the second cycle, basically no formation of new micro-cracks is registered (ε_{res} = -0.01 mm/m, Table 2). Accordingly, SEM observation of W-UT samples revealed no significant formation of new micro-cracks after the two thermal cycles (Figure 2, W-UT-Post).

To evaluate the behavior of the weathered samples consolidated by HAP and the alternative consolidants, the thermal strain as a function of temperature during the first cycle was considered (Figure 6). In Figure 6, the untreated samples (UW-UT and W-UT) are first compared, to evaluate how the initial sample condition influenced its thermal response. Then, the behavior of the consolidated samples is shown in the Figure, reporting also the curves of the UW-UT-2 and W-UT-2 samples, that represent (for the respective conditions) the most extreme cases.

During the first cycle, the W-DAP3M samples exhibited a lower thermal expansion coefficient than the UT-UW samples (α_t = 7.7×10^{-6} instead of 10.8×10^{-6} °C^{-1}), a lower maximum strain (ε_{max} = 0.38 instead of 0.69 mm/m) and a lower residual strain at the end of the cycle (ε_{res} = 0.03 instead of 0.26 mm/m) (Table 2). Actually, the W-DAP3M samples exhibited the lowest residual strain among all the investigated conditions and, for one specimen, a negative residual strain (i.e. a contraction) was measured at the end of the thermal cycle. Although uncommon, contraction of Carrara marble after heating/cooling cycles has been reported in the literature [17]. For the W-DAP3M samples, the lack of significant thermal damage, that would be denoted by a high positive residual strain, can be ascribed to the good adhesion between calcite grains and to the limited pore occlusion achieved after treatment. Both factors are thought to have contributed to achieve a good ability of undergoing thermal expansion and deformation without significant

13

formation of new micro-cracks. This is also suggested by the fact that the W-DAP3M samples, unlike all the other samples, did not experience any dramatic change in α_t, ε_{max} and ε_{res} between the two cycles (Table 2), which is a signal that no dramatic formation of new micro-cracks took place during the cycles. This finds a confirmation also in the results of SEM observation (Figure 3). The largest part of micro-cracks, that had formed after preliminary weathering and that had been healed by HAP, still appears as healed by the consolidant after the thermal cycles ("W-DAP3M-Post", left image). Only a few micro-cracks not filled by HAP (hence presumably formed during the thermal cycles and not during preliminary weathering) can be detected (Figure 3, "W-DAP3M-Post", right image).

The W-DAP0.1M samples exhibited a behavior that was intermediate between the W-UT and the UW-UT references (Figure 6), as indicated also by α_t and ε_{res} values (Table 2). Most of the micro-cracks remained sealed after the thermal cycles (Figure 3, "W-DAP0.1M-Post", left image), even if some new cracks and, in some cases, the rupture of the HAP layer inside the cracks can be noticed (Figure 3, "W-DAP0.1M-Post", right image). In agreement with the previous observation that the treatment did not uniformly improve marble cohesion but caused calcium phosphate formation mainly near the surface, after the thermal cycles several "clean" micro-cracks are visible in the inner part of the samples, which may have formed during preliminary weathering (without being filled with the consolidant) or during the thermal cycles.

The W-AmOx and W-ES samples exhibited a behavior intermediate between the W-UT and the UW-UT samples (Figure 6). Both treatments made the thermal expansion coefficient return to a value similar to that of the UW-UT condition, without making the residual strain exceed the value of the UW-UT reference (Table 2). As for the W-AmOx sample, even if some micro-cracks near the surface still appear as sealed after the thermal cycles (Figure 3, "W-AmOx-Post", left image), most of the micro-cracks, that were originally filled by the consolidant, appear as broadened, so that the consolidant is detached (Figure 3, "W-AmOx-Post", right image). As for the W-ES sample, notwithstanding a few cracks still sealed after the thermal cycles (Figure 3, "W-ES-Post", left

image), in most of the cracks the consolidant appears as sharply torn by further formation of cracks during the thermal cycles, (Figure 3, "W-ES-Post", right image).

Considering that the aim of stone consolidation is to bring stone properties from a condition of weathering (W-UT) back to a condition as similar as possible to that before weathering (UW-UT) [28], all the treatments appear as fairly compatible in terms of thermal behavior after consolidation (Figure 6 7). In particular, none of treatments worsened (i.e. increased) the residual strain after the thermal cycles, compared to the unweathered condition (Table 2), which means that no thermal damage was produced as a consequence of consolidation.

Notably, the W-DAP3M samples exhibited the highest increase in marble cohesion and basically no residual thermal strain after the heating-cooling cycles, hence this treatment appears as the most preferable among those investigated in this study.

4. CONCLUSIONS

In the present study, the thermal behavior of Carrara marble, preliminary artificially weathered by heating at 400 °C and then consolidated by an innovative treatment based on hydroxyapatite, was investigated and compared to two alternative commercial consolidants (ammonium oxalate and ethyl silicate). Based on the obtained results, the following conclusions can be derived:

1) Preliminarily weathered samples exhibited a lower thermal expansion coefficient and a lower residual strain than the unweathered samples, because in pre-weathered marble more micro-cracks are present to accommodate calcite crystals deformation without formation of new micro-cracks.

2) All the investigated treatments caused an increase in thermal expansion coefficient, compared to the weathered untreated reference. This was a consequence of the re-established cohesion between calcite crystals and the partial occlusion of micro-cracks, reducing the so-called

"buffering" effect (i.e. the partial accommodation of calcite crystals deformation made possible by the existing porosity).

3) Considering that consolidation is aimed at bringing the material back to a condition as similar as possible to that before weathering and also considering that none of the treatments caused an increase in residual strain compared to the unweathered condition, all the treatments can be considered as fairly compatible in terms of thermal behavior after consolidation.

4) The HAP-treatment based on application of a 3 M DAP solution was found to cause the highest increase in marble cohesion and no irreversible damage after the thermal cycles. Therefore, this treatment appears as the most preferable among those investigated in this study. The treatments based on ammonium oxalate and ethyl silicate were found to be sufficiently compatible in terms of thermal behavior; however, previous studies highlighted some important issues for these treatments (mainly, the limited efficacy and durability of ammonium oxalate and the limited efficacy and chromatic compatibility of ethyl silicate [16,21,44]), hence the HAP-based treatments seem preferable over these alternative consolidants.

REFERENCES

[1] S. Siegesmund, K. Ullemeyer, T. Weiss, E.K. Tschegg, Physical weathering of marbles caused by anisotropic thermal expansion, Int J Earth Sci 89 (2000) 170-182

[2]   A. Luque, E. Ruiz-Agudo, G. Cultrone, E. Sebastiàn, S. Siegesmund, Direct observation of microcrack development in marble caused by thermal weathering, Environ Earth Sci 62 (2011) 1375-1386

[3]   E. Sassoni, E. Franzoni, Sugaring marble in the Monumental Cemetery in Bologna (Italy): characterization of naturally and artificially weathered samples and first results of consolidation by hydroxyapatite, Appl Phys A-Mater 117 (2014) 1893-1906

[4]   A.E. Charola, S.A. Centeno, K. Normandin, The New York Public Library: Protective treatment for sugaring marble, Journal of Architectural Conservation 16 (2010) 29-44

[5]   G. Royer-Carfagni, Some considerations on the warping of marble façades: The example of Alvar Aalto's Finland Hall in Helsinki, Constr Build Mater 13 (1999) 449-457

[6]   S. Siegesmund, J. Ruedrich, A. Koch, Marble bowing: comparative studies of three different public building facades, Environ Geol 56 (2008) 473-494

[7]   E. Franzoni, E. Sassoni, Correlation between microstructural characteristics and weight loss of natural stones exposed to simulated acid rain, Sci Total Environ 412-413 (2011) 278-285

[8]   K. Malaga-Starzec, U. Åkesson, J.E. Lindqvist, B. Schouenborg, Microscopic and macroscopic characterization of the porosity of marble as a function of temperature and impregnation, Constr Build Mater 20 (2006) 939-947

[9]   D. Pinna, B. Salvadori, S. Porcinai, Evaluation of the application conditions of artificial protection treatments on salt-laden limestone and marble, Constr Build Mater 25 (2011): 2723-2732

[10]   G.S. Wheeler, S.A. Fleming, S. Ebersole, Evaluation of some current treatments for marble, In: La conservation des monuments dans le bassin mediterraneen: Actes du 2° symposium international, Geneve, 19-21/11/1991, 1992, 439-443

[11]   V. Verges-Belmin, G. Orial, D. Garnier, A. Bouineau, R. Coignard, Impregnation of badly decayed Carrara marble by consolidating agents: Comparison of seven treatments, In: La conservation des monuments dans le bassin metiterraneen: Actes du 2° symposium international, Geneve, 19-21/11/1991, 1992, 421-437

[12]   T. Poli, L. Toniolo, O. Chiantore, The protection of different Italian marbles with two partially flourinated acrylic copolymers, Appl Phys A-Mater 79 (2004) 347-351

[13] T. Skoulikidis, P. Vassiliou, K. Tsakona, Surface consolidation of Pentelic marble - Criteria for the selection of methods and materials - The Acropolis case, Environ Sci & Pollut Res 12 (2005) 28-33

[14] G.S. Wheeler, Alkoxysilanes and the Consolidation of Stone (Research in conservation), The Getty Conservation Institute, Los Angeles, 2005

[15] M. Matteini, Inorganic treatments for the consolidation and protection of stone artefacts, Conservation Science in Cultural Heritage 8 (2008) 13-27

[16] E. Sassoni, G. Graziani, E. Franzoni, Repair of sugaring marble by ammonium phosphate: comparison with ethyl silicate and ammonium oxalate and pilot application to historic artifact, Materials and Design 88 (2015) 1145-1157

[17] J. Ruedrich, T. Weiss, S. Siegesmund, Thermal behavior of weathered and consolidated marbles, In: Siegesmund S., Weiss T., Vollbrecht A., Natural stone, weathering phenomena, conservation strategies and case studies, Geological Society, London, Special Publications, 205 (2002) 255-271

[18] E. Sassoni, S. Naidu, G.W. Scherer, The use of hydroxyapatite as a new inorganic consolidant for damaged carbonate stones, J Cult Herit, 12 (2011) 346-355

[19] S. Naidu, G.W. Scherer, Nucleation, growth and evolution of calcium phosphate films on calcite, Journal of Colloidal and Interface Science 435 (2014) 128-137

[20] S. Naidu, J. Blair, G.W. Scherer, Acid-Resistant Coatings on Marble, Journal of the American Ceramic Society (in press), DOI: 10.1111/jace.14355

[21] G. Graziani, E. Sassoni, E. Franzoni, G.W. Scherer, Hydroxyapatite coatings for marble protection: Optimization of calcite covering and acid resistance, Applied Surface Science 368 (2016) 241-257

[22] F. Yang, B. Zhang, Y. Liu, W. Guofeng, H. Zhang, W. Cheng, Z. Xu, Biomimic conservation of weathered calcareous stones by apatite, New J Chem 35 (2011) 887-892

[23] M. Matteini, S. Rescic, F. Fratini, G. Botticelli, Ammonium phosphates as consolidating agents for carbonatic stone materials used in architecture and cultural heritage: Preliminary research, Int J Archit Herit, 5 (2011) 717-736

[24] Q. Liu, B. Zhang, Synthesis and characterization of a novel biomaterial for the conservation of historic stone building and sculptures, Mater Sci Forum 675-677 (2011) 317-320

[25]   E. Sassoni, E. Franzoni, B. Pigino, G.W. Scherer, S. Naidu, Consolidation of calcareous and siliceous sandstones by hydroxyapatite: comparison with a TEOS-based consolidant, Journal of Cultural Heritage 14S (2013) e103-e108

[26]   F. Yang, Y. Liu, Artificial hydroxyapatite film for the conservation of outdoor marble artworks, Materials Letters 124 (2014) 201–203

[27]   S. Naidu, C. Liu, G.W. Scherer, New techniques in limestone consolidation: Hydroxyapatite-based consolidant and the acceleration of hydrolysis of silicate-based consolidants, Journal of Cultural Heritage 16 (2015) 94-101

[28]   E. Sassoni, G. Graziani, E. Franzoni, An innovative phosphate-based consolidant for limestone. Part 1: Effectiveness and compatibility in comparison with ethyl silicate, Construction and Building Materials 102 (2016) 918-930

[29]   E. Sassoni, G. Graziani, E. Franzoni, An innovative phosphate-based consolidant for limestone. Part 2: Durability in comparison with ethyl silicate, Construction and Building Materials 102 (2016) 931-942

[30]   E. Possenti, C. Colombo, D. Bersani, M. Bertasa, A. Botteon, C. Conti, P.P. Lottici, M. Realini, New insight on the interaction of diammonium hydrogenphosphate conservation treatment with carbonatic substrates: A multi-analytical approach, Microchemical Journal 127 (2016) 79–86

[31]   H2020-MSCA-IF-2014-GF Project HAP4MARBLE, "Multi-functionalization of hydroxyapatite for restoration and preventive conservation of marble artworks" (Marie Sklodowska-Curie grant agreement No 655239), https://events.unibo.it/hap4marble

[32]   E. Sassoni, E. Franzoni, Consolidation of Carrara marble by hydroxyapatite and behaviour after thermal ageing, In: Toniolo L. et al. (Eds), Built Heritage: Monitoring Conservation Management, Research for Development, Springer International Publishing, 2015, p. 379-389, DOI: 10.1007/978-3-319-08533-3_32

[33]   E. Franzoni, E. Sassoni, G.W. Scherer, S. Naidu, Artificial weathering of stone by heating, Journal of Cultural Heritage 14S (2013) e85-e93

[34]   E. Sassoni, E. Franzoni, Influence of porosity on artificial deterioration of marble and limestone by heating, Appl Phys A-Mater 115 (2014) 809–816

[35] C. Conti, C. Colombo, G. Festa, J. Hovind, E.P. Cippo, E. Possenti, M. Realini, Investigation of ammonium oxalate diffusion in carbonatic substrates by neutron tomography, J Cult Herit, DOI: 10.1016/j.culher.2015.12.005

[36] G.W. Scherer, G.S. Wheeler, Silicate consolidants for stone, Key Eng Mater 391 (2009) 1-25

[37] E. Franzoni, E. Sassoni, G. Graziani, Brushing, poultice or immersion? Role of the application technique on the performance of a novel hydroxyapatite-based consolidating treatment for limestone, Journal of Cultural Heritage 16 (2015) 173–184

[38] E. Sassoni, G. Graziani, G.W. Scherer, E. Franzoni, Some recent findings on marble conservation by aqueous solutions of diammonium hydrogen phosphate, MRS Advances (in press)

[39] M. Matteini, A. Moles, S. Giovannoni, Calcium oxalate as a protective mineral system for wall paintings: methodology and analyses, In: V. Fassina, H. Ott, F. Zezza (Eds) III Int. Symp. Conservation of Monuments in the Mediterranean Basin, 1994

[40] E. Franzoni, G. Graziani, E. Sassoni, TEOS-based treatments for stone consolidation: acceleration of hydrolysis-condensation reactions by poulticing, Journal of Sol-Gel Science and Technology, 74 (2015) 398-405

[41] T. Weiss, P.N.J. Rasolofosaon, S. Siegesmund, Ultrasonic wave velocities as a diagnostic tool for the quality assessment of marble, In: Siegesmund S., Weiss T., Vollbrecht A., Natural stone, weathering phenomena, conservation strategies and case studies, Geological Society, London, Special Publications, 205 (2002) 149-164

[42] M. Pamplona, S. Simon, Ultrasonic pulse velocity - A tool for the condition assessment of outdoor marble sculptures, Proceedings of 12th International Congress on Deterioration and Conservation of Stone, New York City (USA), 22-26 October 2012, p. 1-13, http://iscs.icomos.org/pdf-files/NewYorkConf/pampsimo.pdf

[43] E. Lerner, R. Azoury, S. Sarig, Rapid precipitation of apatite from ethanol-water solution, Journal of Crystal Growth 97 (1989) 725-730

[44] G. Wheeler, Alkoxysilanes and the consolidation of stone, The Getty Conservation Institute, Los Angeles, 2005

[45] A. Zeisig, S. Siegesmund, T. Weiss, Thermal expansion and its control on the durability of marbles, Geological Society Special Publication 205 (2002) 65-80

Table 1. Ultrasonic pulse velocity (UPV) of untreated and treated samples (UW-UT = unweathered, untreated; W-UT = weathered, untreated; W-DAP3M = weathered, treated with 3M DAP solution; W-DAP0.1M = weathered, treated with 0.1 M DAP solution; W-AmOx = weathered, treated with ammonium oxalate; W-ES = weathered, treated with ethyl silicate). Values are averages for 2 samples (difference from maximum/minimum values in brackets.

	UW-UT	W-UT	W-DAP3M	W-DAP0.1M	W-AmOx	W-ES
UPV (km/s)	3.2 (±0.1)	0.6 (±0.0)	2.9 (±0.1)	2.2 (±0.1)	2.3 (±0.1)	2.1 (±0.1)

Table 2. Thermal expansion coefficient (α_t) between 35 and 60 °C, maximum strain at 80 °C (ε_{max}) and residual strain at 35 °C (ε_{res}) of untreated and treated samples subjected to thermal cycles (UW-UT = unweathered, untreated; W-UT = weathered, untreated; W-DAP3M = weathered, treated with 3M DAP solution; W-DAP0.1M = weathered, treated with 0.1 M DAP solution; W-AmOx = weathered, treated with ammonium oxalate; W-ES = weathered, treated with ethyl silicate). Values are averages for 2 samples (difference from maximum/minimum values in brackets.

|	$\alpha_t \times 10^{-6}$ (°C^{-1})		ε_{max} (mm/m)		ε_{res} (mm/m)	
	1st cycle	2nd cycle	1st cycle	2nd cycle	1st cycle	2nd cycle
UW-UT	10.8 (±0.4)	9.5 (±2.0)	0.69 (±0.05)	0.46 (±0.09)	0.26 (±0.05)	0.06 (±0.01)
W-UT	3.0 (±0.9)	2.0 (±1.6)	0.26 (±0.01)	0.12 (±0.02)	0.10 (±0.03)	-0.01 (±0.02)
W-DAP3M	7.7 (±1.7)	7.7 (±1.8)	0.38 (±0.06)	0.36 (±0.08)	0.03 (±0.01)	0.00 (±0.01)
W-DAP0.1M	10.5 (±2.6)	8.9 (±1.2)	0.52 (±0.06)	0.32 (±0.03)	0.16 (±0.01)	0.01 (±0.01)
W-AmOx	11.0 (±0.2)	10.2 (±0.2)	0.60 (±0.00)	0.43 (±0.04)	0.16 (±0.01)	0.02 (±0.02)
W-ES	6.4 (±0.4)	6.7 (±1.2)	0.46 (±0.02)	0.27 (±0.04)	0.23 (±0.01)	0.02 (±0.00)

Figure 1. Examples of thermally induced degradation of marble. Left: Marble columns in the Courtyard of the Lions in the Alhambra of Granada (Spain, XIV century) exhibit severe granular disaggregation in the side directly exposed to solar radiation, while in the opposite sheltered side the same columns are substantially well preserved. Right: Thin slabs used as gravestones in the *Père Lachaise* Cemetery in Paris (France, XIX century) exhibit dramatic bowing and deformation.
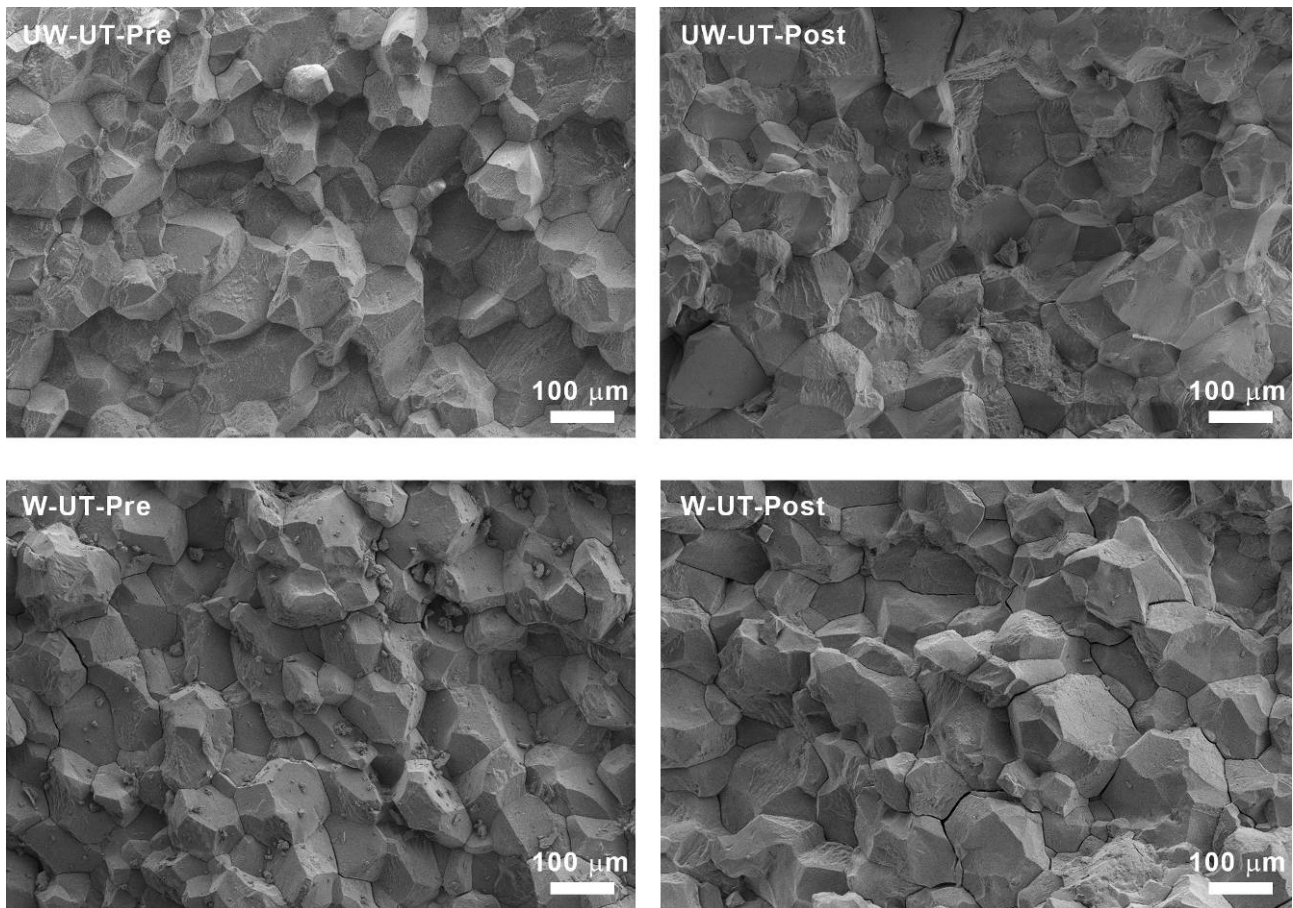
**Figure 2**. SEM images of untreated samples before ("-Pre") and after ("-Post") the thermal cycles.
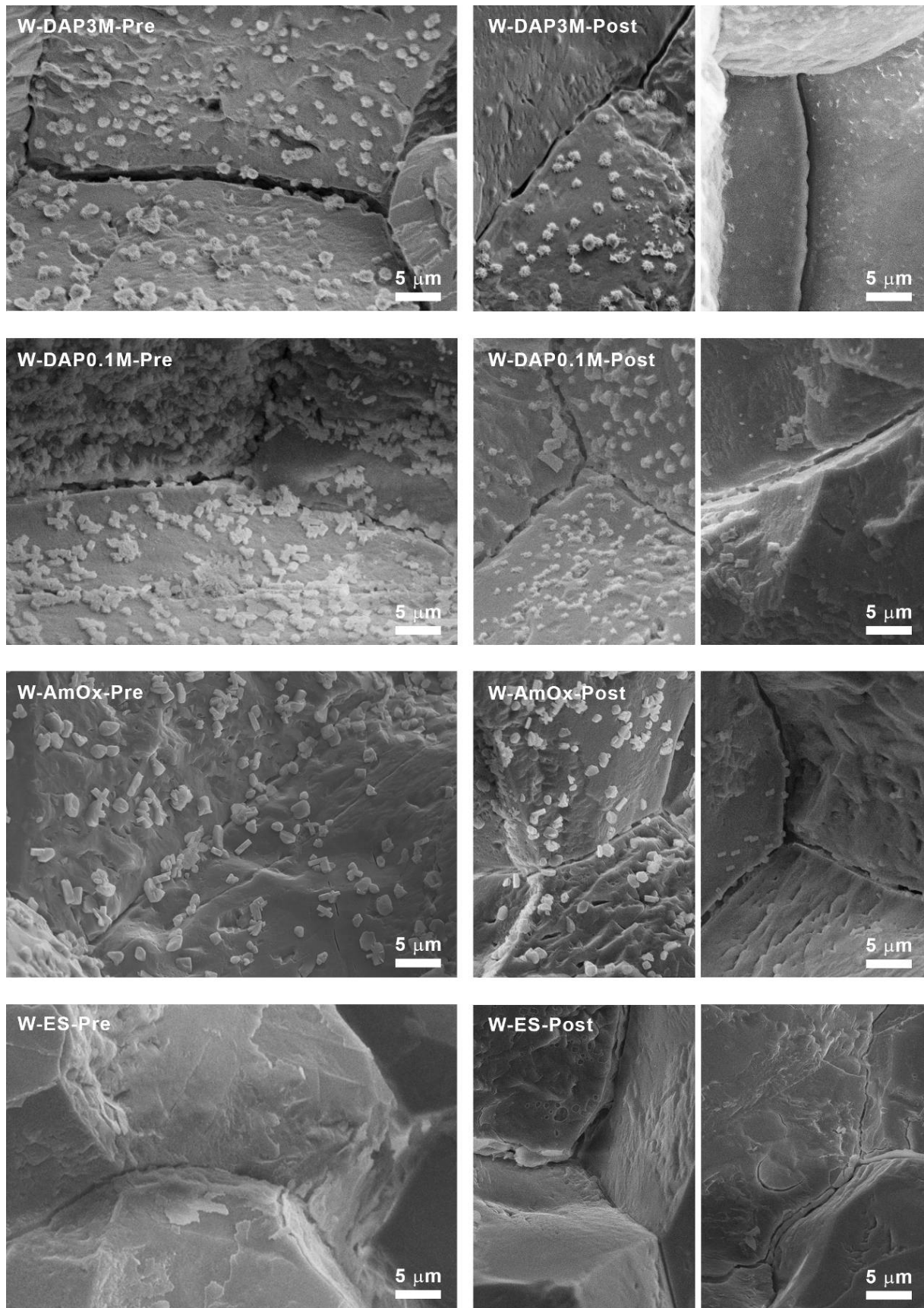
Figure 3. SEM images of treated samples before ("-Pre") and after ("-Post") the thermal cycles. In samples already subjected to thermal cycles, different conditions are illustrated ("-Post" condition, left and right images).
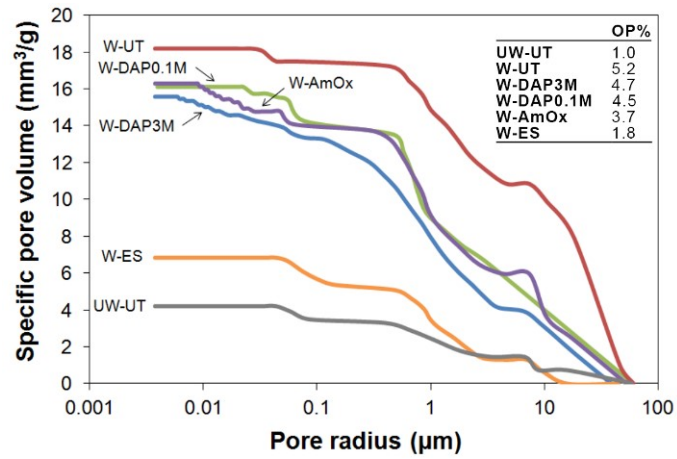
Figure 4. Pore size distribution and open porosity (*OP*) of untreated and treated samples.
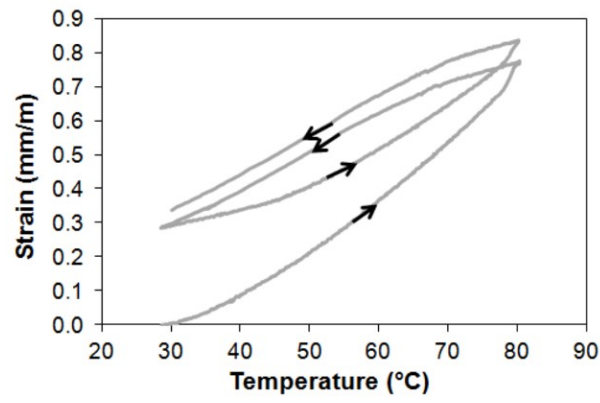
Figure 5. First and second thermal cycle for the unweathered, untreated sample UW-UT-2.
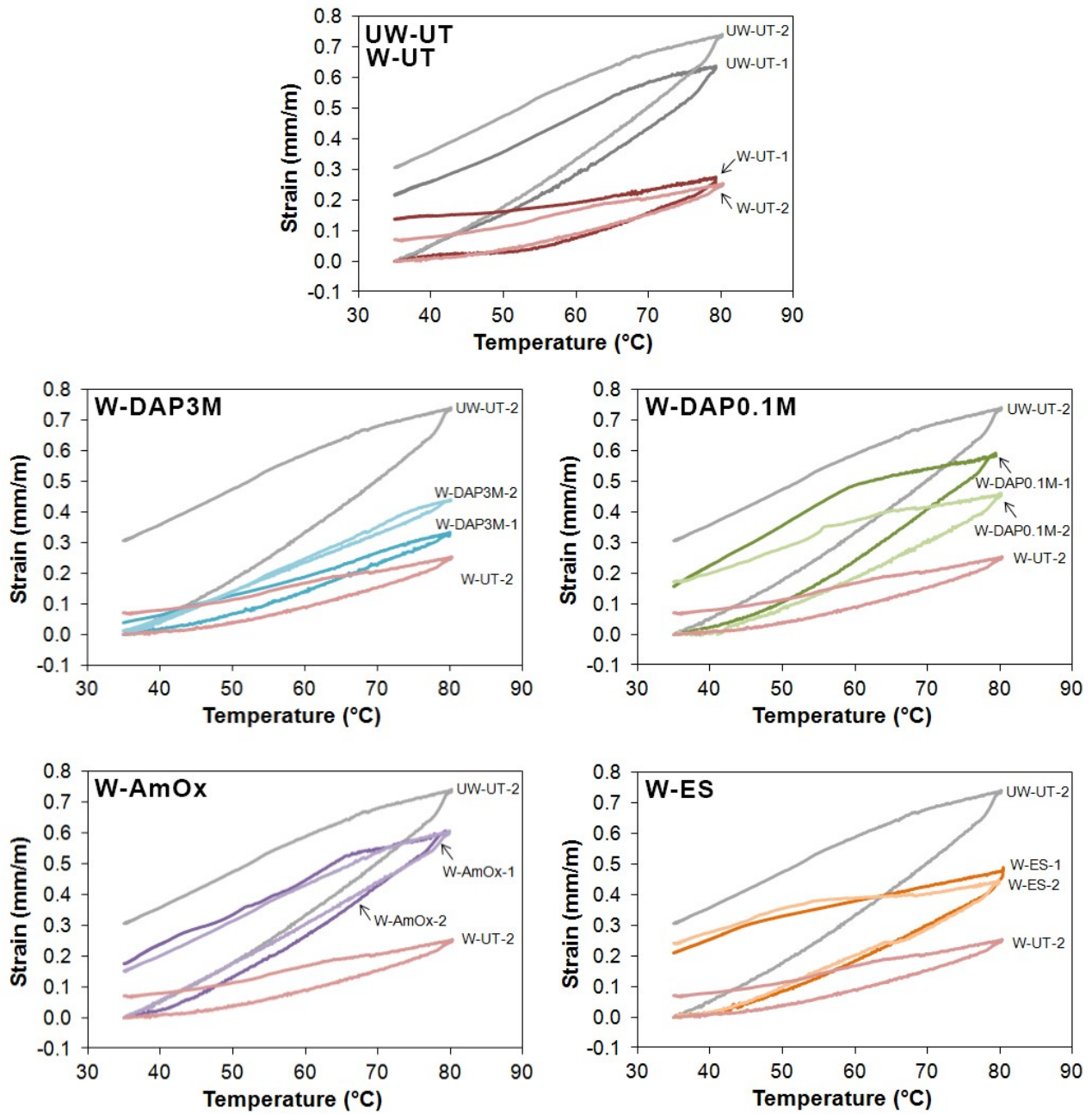
Figure 6. Thermal strain as a function of temperature for untreated and treated samples during the first thermal cycle.